RESEARCH ARTICLE

Variation of functional brain connectivity in epileptic seizures: an EEG analysis with cross-frequency phase synchronization

Haitao Yu[1] · Lin Zhu[1] · Lihui Cai[1] · Jiang Wang[1] · Chen Liu[1] · Nan Shi[2] · Jing Liu[2]

Abstract

Frequency coupling in nervous system is believed to be associated with normal and impaired brain functions. However, most of the existing experiments have been concentrated on the coupling strength within frequency bands, while the coupling strength between different bands is ignored. In this work, we apply phase synchronization index (PSI) to investigate the cross-frequency coupling (CFC) of Electroencephalogram (EEG) signals. The PSI matrixes for the multi-channel EEG signals are calculated from interictal to ictal period in each sliding time window. The results show that CFC changes obviously once seizure occurs between the different bands, and such alteration is earlier than the appearance of clinical symptoms in seizure. Considering the similar role of the within-frequency coupling (WFC), we further reconstruct multi-layered brain networks, including CFC networks and WFC networks. The graph metrics are applied to investigate the variation of network structure of the epileptic brain. Significant decreases/increases of the local/global efficiency are found in δ–β, δ–α, θ–α and δ–θ bands from the CFC network, while WFC network shows a significant decline in the local efficiency in θ and α bands. These findings suggest that CFC may provide a new perspective to observe the alteration of brain structure when seizure occurs, and the investigation of functional connectivity across the full frequency spectrum can give us a deeper understanding of epileptic brains.

Keywords Cross-frequency coupling · Phase synchronization index · Functional brain network · Synchronization · Epilepsy

Introduction

Epilepsy is a chronic neurological disease characterized by paroxysmal abnormal electrical discharges of neurons in the brain (Roper and Yachnis 2002). According to the latest epidemiological data, there are about 50 million people affected by epilepsy globally, and nearly 30% patients cannot be controlled with anticonvulsive medication and surgery (Greter et al. 2018). The unpredictable epileptic seizures may cause permanent damage to patient's brain and increase the risk of accidental injuries as a result of losing control of their bodies during seizure. Electroencephalogram

(EEG), as a technique monitoring the electrophysiological activities, has proved to be an effective tool in investigating brain function with the nature of non-invasion and high time resolution (Mormann et al. 2000; Abasolo et al. 2005). The scalp EEG shows a drastic increase in amplitude and shows sharp wave, spike wave or spike (or sharp) slow wave complex during ictal state, and thus is considered as a preferred tool to detect the seizures (Iasemidis et al. 2003; Benbadis and Allen Hauser 2000). However, the accurate diagnosis of epilepsy that is based on the visual inspection of continuous temporal EEG waveform usually requires several days of EEG monitoring, and is tedious, time-consuming and prone to human error (Tetzlaff et al. 2003; Medvedev et al. 2011; Martis et al. 2013; Donos et al. 2015; Hortal et al. 2016; Yuan et al. 2018). Therefore, we need to propose a new, more discriminative feature for the diagnosis of epilepsy.

Epileptic seizures are related to the excessive synchronization or abnormal activities in the brain cortex and such abnormal synchrony dynamics in the brain can affect

✉ Chen Liu
  liuchen715@tju.edu.cn

[1] School of Electrical and Information Engineering, Tianjin University, Tianjin, China

[2] Department of Neurology, Tangshan Gongren Hospital, Tangshan 063000, Hebei, China

function connectivity and information transmission within and cross different brain regions (Percha et al. 2005; Tecchio et al. 2018). The current research on epilepsy that is based on phase synchronization of scalp EEG mainly focuses on the interaction between different leads within a single frequency band (Amiri et al. 2016). However, the importance of investigation on cross-frequency coupling (CFC) is growing (Zheng and Zhang 2013; Nishida et al. 2014) and correlation models that is based on the selection of single band are considered as incomplete. Although the CFC is indeed much weaker than the within frequency coupling (WFC), CFC may indeed play an important role in the result of electrophysiological studies through the correlation models consisting of both WFC and CFC. Canolty and Knight (2010) accounted for CFC might serve as a mechanism to transfer information from large-scale brain networks operating at behavioral timescales to the fast, local cortical processing required for effective computation and synaptic modification, thus integrating functional systems across multiple spatiotemporal scales. In addition, CFC has proved to be associated with the attack and progression of neurological disorders such as epilepsy. Villa and Tetko (2010) used the index of resonance to measure the CFC and found that the coupling strength varied with the changes triggered by the circuits involved in the initiation of the epileptic seizures. In addition, some rodent experiments revealed that CFC was stronger in the seizure onset zones (Nariai et al. 2011; Weiss et al. 2013; Ibrahim et al. 2014; Amiri et al. 2016), and during the pre-ictal and ictal phases (Samiee et al. 2018). Such studies suggested that the CFC measures might also be a good biomarker for detecting seizure onset and termination (Guirgis et al. 2015; Malladi et al. 2018; Jacobs et al. 2018).

Over the past decade, the brain is gradually seen as a complex network with dynamic interactions between local and further remote brain regions (Wang and Meng 2016). Since studying on the single feature of electrophysiological signal is regarded as insufficient, the measurement of brain functional network parameters is becoming a focus in many neurological studies, and it has a rapid development in the network analysis based on EEG (Biswal et al. 1995; Buckner et al. 2009). Moreover, growing evidence shows that the network properties are altered in neurological disorders such as Alzheimer's disease, Parkinson's disease and epilepsy (Apkarian et al. 2005; Rogasch and Fitzgerald 2013). Ponten et al. (2007, 2009) have found that functional neural network changed during epileptic seizures and the network became more regular in weighted and unweighted analyses, compared to the more random pre-ictal network configuration. Adebimpe et al. also found that the benign epileptic brain networks showed functionally disrupted patterns compared to healthy controls. Recently,

a framework of multi-layer network has been developed, combining the within- and cross- frequency interactions (Adebimpe et al. 2016). Müller et al. (2016) constructed a hyper-frequency network across the spectrum from 2 to 20 Hz, and found that the network showed temporal and topological changes during rest and stimulus processing state. Cai et al. (2018) found that the properties of network based on CFC were altered compared to the normal controls. Hence, the multi-layer network analysis may also benefit our understanding about the etiological mechanism of epilepsy.

The conventional automatic detection of EEG recordings is generally dependent on the examination of the linear features like frequency or wavelength, voltage or amplitude, waveform regularity, and reactivity to eye opening (Kirmani 2013; Jiang et al. 2017). While in recent years, a growing attention is paid to the nonlinear and nonstationary properties of electrophysiology signal like scalp EEG (Kannathal et al. 2005; Zhang et al. 2015). Nonlinear features such as fractal dimension, Lempel–Ziv complexity, entropy have been extracted from complex electrophysiology signals, and applied to the analysis and diagnosis of neurological diseases. For instance, Kannathal et al. (2005) proved that entropy estimators can distinguish normal and epileptic EEG data with more than 95% confidence. Zhang et al. (2015) estimated the fractal dimensions of preprocessed EEG and applied this feature into seizure detection. Based on this, an average sensitivity of 94.05% can be achieved. These methods are all used to study the nonlinear characters of a single channel. However, the brain is a delicate organ to realize the separation and integration of the information. There are interactions between the different brain regions. Therefore, the relationship between the EEG signals of different channels should also be considered. Analyzing the brain functional connectivity and the neural synchronization facilitates the exploration of the pathological neuronal synchronization associated with the neurological diseases (Mormann et al. 2000; Lo 2010; Qu et al. 2012). Phase synchronization index (PSI), as a quantification index, can describe the features of two time-series of neurophysiological signals, which has been used in EEG analysis recently (Wacker and Witte 2011; Belluscio et al. 2012; Zheng and Zhang 2013; Szymanski et al. 2017). For instance, Edakawa et al. (2016) found a strong coupling exists between the phase of β (12–35 Hz) and the amplitude of high γ (35–200 Hz) frequency bands. However, most of the existing PSI-based studies focused on the difference between epileptic patients and normal controls, which ignored the change trends of synchronization strength during seizures. Based on the definition of PSI, we use PSI to estimate the coupling changes from the EEG signals in the different channels during serizures.

Thus, in this work, we concentrate on the variation of functional brain connectivity within and between different frequency bands during a period of time near the onset. Firstly, the original scalp EEGs are divided into four frequency bands: δ (0–3.75 Hz), θ (3.75–7.5 Hz), α (7.5–15 Hz) and β (15–30 Hz). Then we apply PSI to quantify the connectivity strength between different regions across the four frequency bands, with both CFC and WFC being considered. Finally, we construct a multi-layer functional brain network based on the PSI matrixes and explore the abnormal network properties for epilepsy by estimating global efficiency, local efficiency and small world characteristic based on graph theory.

Experiment design and EEG recording

Subjects information

This work uses the CHB-MIT scalp EEG dataset which were contributed by Children's Hospital Boston (CHB) and the Massachusetts Institute of Technology (MIT). These recordings were collected from 22 subjects (5 males of ages between 3 to 22 years and 17 females of ages between 1.5 to 19 years). For each subject, the EEG signals were sampled at 256 Hz with 16-bit quantization and each channel of the EEG data was obtained by the potential difference between two different electrodes. Most cases contain 23 bipolar EEG signals while a few cases contain less or more channels. Therefore, only the onset records that contain the 23 EEG channels (FP1-F7, F7-T7, T7-P7, P7-O1, FP1-F3, F3-C3, C3-P3, P3-O1, FZ-CZ, CZ-PZ, FP2-F4, F4-C4, C4-P4, P4-O2, FP2-F8, F8-T8, T8-P8, P8-O2, P7-T7, T7-FT9, FT9-FT10, FT10-T8, T8-P8) was selected to keep the samples uniform (the chb15 was excluded, and the information of the remaining epileptics is shown in Table 1). The location to place electrodes is shown in the Fig. 1a.

Preprocessing

To concentrate on the change of epileptic brain near seizure, we first select 120 s-length (60 s before and 60 s after the seizure onset) EEG data for each seizure. Previous study showed that most brain activity occurred between 0 and 30 Hz (Adebimpe et al. 2016), and changes in EEG during seizure might occur in multiple frequency components. Therefore, we decompose each channel of selected EEG data into four sub-bands: δ, θ, α and β by a band-passed finite impulse digital filter that based on fast Fourier transform (Salvador et al. 2005). A sliding window is applied to each session of EEG recordings to split the signals into segments to investigate the occasion that the

Table 1 Patients Information of CHB-MIT EEG Database

Subject	Gender	Age (years)	Total seizure number
chb01	F	11	6
chb02	M	11	3
chb03	F	14	7
chb04	M	22	4
chb05	F	7	4
chb06	F	1.5	9
chb07	F	14.5	3
chb08	M	3.5	4
chb09	F	10	4
chb10	M	3	6
chb11	F	12	3
chb12	F	2	26
chb13	F	3	12
chb14	F	9	8
chb16	F	7	10
chb17	F	12	3
chb18	F	18	6
chb19	F	19	3
chb20	F	6	8
chb21	F	13	4
chb22	F	9	3
chb23	F	6	7

change of synchronization. In order to achieve high confidence of the data, the EEG data is segmented into 3 s epochs with 2 s overlap.

Method

Phase synchronization index

Phase Synchronization Index (PSI) is utilized to quantify the phase coupling strength within and between different frequency bands. To compute the PSI, we apply Hilbert transform (Thuraisingham et al. 2012) to extract the instantaneous phase of all electrodes from the original EEG data. Let $x(t)$ be a real-valued signal and let $\tilde{x}(t)$ be the Hilbert transform of $x(t)$ defined by

$$\tilde{x}(t) = \frac{1}{\pi} p \cdot v \cdot \int_{-x}^{\infty} \frac{x(\tau)}{t - \tau} d\tau \tag{1}$$

where $p \cdot v$ denotes that the transform is defined using the Cauchy principal value. Then both the instantaneous amplitude $A(t)$ and the instantaneous phase $\varphi(t)$ can be computed by:
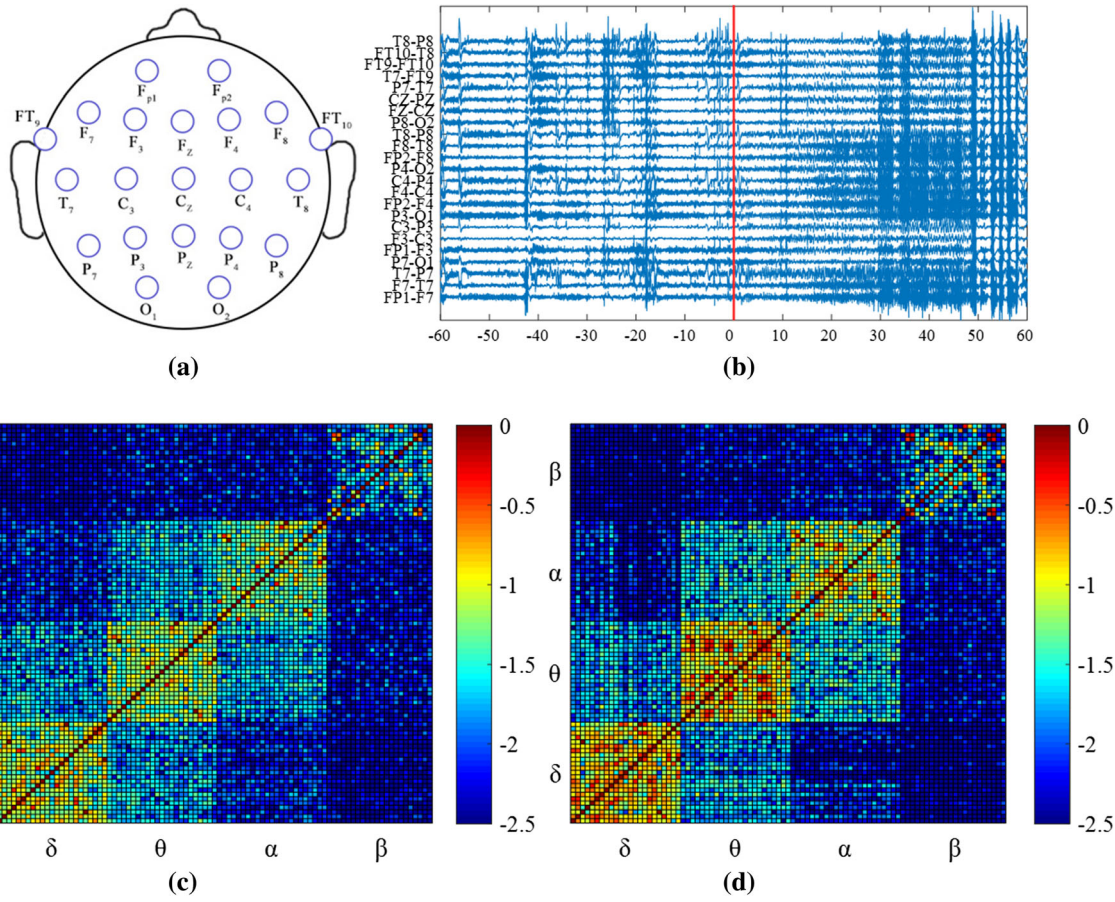
Fig. 1 Cross frequency synchronization before and after seizure onset. **a** Diagram of electrode placement; **b** 120 seconds time series raw EEG signals while the seizure onset (60 seconds) is marked with red line; **c–d** the (logarithmic) synchronization matrices for 10s-20s (**c**) and 70s-80s (**d**) section

$$\begin{cases} A(t) = \sqrt{[x(t)]^2 + [\tilde{x}(t)]^2} \\ \varphi(t) = \arctan\dfrac{\tilde{x}(t)}{x(t)} \end{cases} \tag{2}$$

The phase difference between the two signals is defined as:

$$\Delta\varphi(f_m, f_n, t) = m\varphi(f_m, t) - n\varphi(f_n, t) \tag{3}$$

where f_m and f_n are the center frequencies of two signals. Besides, m and n are integers that should satisfy the condition $m \cdot f_n = n \cdot f_m$. In the WFC case with f_m and f_n, the phase difference is calculated by setting $m = n = 1$. The PSI can be defined as

$$PSI(f_m, f_n) = \left| \left\langle e^{j-(\Delta\varphi(f_m, f_n, t))} \right\rangle \right| \tag{4}$$

Graph theoretical analysis

Previous researches have shown that the functional brain networks in epilepsy patients are obviously different from healthy controls (Jeong et al. 2014; Wang and Meng

2016). PSI was required for the construction of adjacency matrix and functional network. Each row (column) of the matrix represented a channel of EEG, and each entry of the matrix was defined by the connectivity between two different nodes. To transform the PSI matrix into the adjacency matrix, a certain percentage of the strongest connections will be retained, and we define the preserved connection between node A and node B as 1, where A and B belong to the 23 bipolar EEG signals as mentioned above. Besides, the selection of the threshold value needs to ensure that there is no isolated node in constructed network. Note that the coupling strength shows great differences between WFC and CFC, therefore we apply the transformation to each 23 × 23 PSI matrix.

The human brain is divided into different brain regions, and each is responsible for processing specific information. Such mechanisms make sure that the brain can process complex information and multiple instructions at the same time. Local efficiency can directly reflect the segregation index of a network. Local efficiency of node i is defined as

$$locE(i) = \frac{1}{N_{G_i}(N_{G_i} - 1)} \cdot \sum_{j \neq k \in G_i} \frac{1}{l_{j,k}} \quad (5)$$

where G_i is the subgraph constituted by the neighbor nodes of node i; j and k are the numbers of nodes which are different with each other in G_i, $l_{j,\ k}$ is the shortest path length between node j and k. Local efficiency of the whole network is defined as

$$locE = \frac{1}{N} \cdot \sum_i locE(i) \quad (6)$$

Considering that single brain regions perform only basic functions while advanced functions require multiple brain regions to cooperate, integration of information from different brain regions is essential. Global efficiency is calculated to measure the integration properties, which is defined as

$$gE = \frac{1}{N(N-1)} \cdot \sum_{i,j \in V, i \neq j} \frac{1}{l_{i,j}} \quad (7)$$

It has been shown that regular networks have both higher clustering coefficient and longer shortest path length (Ponten et al. 2007; Liao et al. 2010). In contrast, random networks have a lower clustering coefficient and a shorter shortest path length. Networks with both high clustering coefficient and short shortest path length are called "small-world network" (Srinivas et al. 2007). The small-world property suggests that brain network is a complex system with both integration and separation functions, and can be measured by combining the local and global efficiency.

Multivariate analysis

The mean PSI of every 23×23 matrix arranged in chronological window is calculated and further averaged separately in two sections: before seizure onset (BSO) and after seizure onset (ASO). One-way Analysis of Variance (ANOVA), as a the analysis method of variance and covariance, is utilized to assess the level of distinguishing different in PSI features, and each sample is obtained by averaging the mean PSI value, which is acquired by averaging the PSI matrix, of all-time windows of once onset in each state (before or after seizure onset) of a single subject. P is a scalar value returned by ANOVA analysis, which describes the degree of difference for all the subject. In this work, we assume there is a great difference between two states (before and after seizure onset) when $P < 0.01$.

Results

The brain activity of epileptic is recorded through multiple-channel bipolar lead system, and Fig. 1b clearly shows 60 s-length EEG signal before and after seizure onset. We use a sliding time window of 3 s length. After frequency division of each EEG segment, we calculate the PSI for each pair-wise channel between and within frequency bands to investigate the change of synchronization in epileptic brain. One PSI value is obtained for each time window. Typical matrixes for one epileptic before and after seizure onset are shown in Fig. 1c, d, respectively. The PSI matrix includes 4 WFC sub-matrixes (the 23×23 connectivity matrices on the diagonal) and 12 CFC sub-matrixes (the 23×23 connectivity matrices on the off-diagonals). Obviously, the strength of WFC is much higher than that of CFC. Moreover, it is observed that WFC is increased during seizure, and also in partial CFC sub-matrixes. We further perform statistical analysis for both WFC and CFC to get the differences before and after seizure onset. The mean of each 23×23 matrix is computed and further respectively averaged over all windows before and after seizure onset. The obtained results are shown in the Table 2. For the CFC, the synchronization level between δ–β and δ–α couplings are significantly increased during seizure, while that between θ–α coupling is decreased. For the WFC, the synchronization levels in δ, θ and α bands are increased obviously. It is demonstrated that the phase synchronization between leads of most different frequency bands changes significantly in epileptic seizure.

We further explore the distribution of PSI values to investigate the variation trend of synchronization level between different brain areas in epileptic seizure. We consider CFC and WFC respectively, and the results of a typical subject are shown in Fig. 2. Before seizure onset, CFC is mainly within the range [0.06, 0.21] and shows a unimodal distribution with single peak at around 0.1 (Fig. 2a). However, during seizure, CFC is within the range [0.05 0.25] and shows a multimodal distribution, which has three peaks at around 0.08, 0.11 and 0.19 (Fig. 2b). The

Table 2 The statistical analysis and the one-way ANOVA results (P values) for the mean synchronization strength, which is obtained by averaging the mean PSI value of PSI matrix of all-time windows respectively before seizure onset (BSO) and after seizure onset (ASO)

	PSI value (BSO)	PSI value (ASO)	P values
δ–β	$0.081 \pm 4.7e - 05$	$0.073 \pm 1.1e - 04$	0.0022 (*)
θ–β	$0.099 \pm 9.1e - 05$	$0.097 \pm 2.6e - 05$	0.3961
α–β	$0.107 \pm 8.9e - 05$	$0.105 \pm 1.1e - 05$	0.5941
δ–α	$0.122 \pm 2.4e - 04$	$0.110 \pm 2.2e - 04$	0.0065 (*)
θ–α	$0.188 \pm 1.4e - 04$	$0.208 \pm 2.8e - 04$	$1.1e - 05$ (*)
δ–θ	$0.177 \pm 2.3e - 04$	$0.172 \pm 2.4e - 04$	0.22
β	0.234 ± 0.0010	$0.250 \pm 6.9e - 04$	0.0443
α	$0.328 \pm 7.3e - 04$	$0.356 \pm 9.8e - 04$	0.0011 (*)
θ	$0.360 \pm 4.4e - 04$	0.424 ± 0.0012	$8.9e - 11$ (*)
δ	$0.398 \pm 8.6e - 04$	0.429 ± 0.0013	0.0013 (*)

*$P < 0.01$ denotes a significant difference
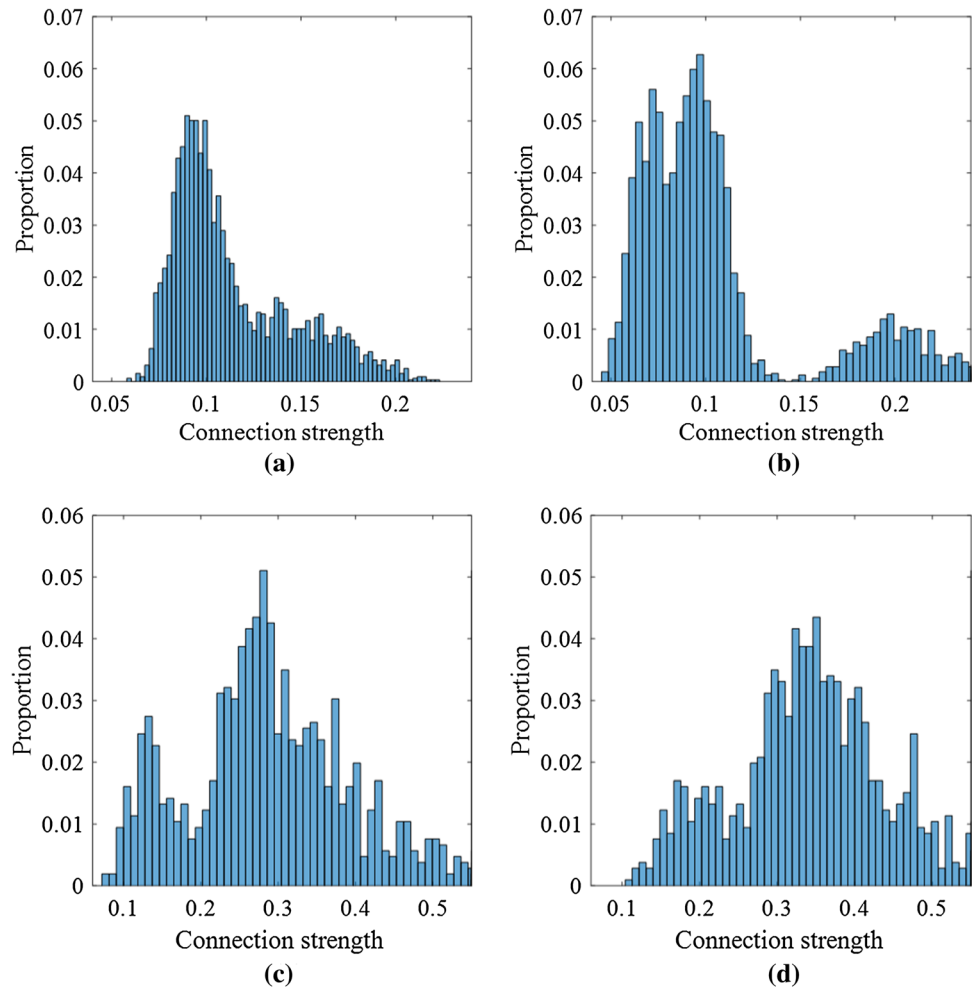
small values of CFC mainly locate in δ–β, θ–β, α–β and δ–α coupling, and the high CFC values mainly locate in θ–α, and δ–θ coupling. According to Table 2, the variation of CFC distribution may be due to the increase of high synchronization level in θ–α coupling and the decrease of low synchronization level in δ–β and δ–α couplings. For the WFC, its value is generally higher and more widely distributed than CFC, as shown in Fig. 2c, d. The distributions of WFC are both bimodal before and after seizure onset, while the range changes from [0.08 0.56] to [0.12 0.56]. The peaks are at 0.12 and 0.28 before seizure onset and at 0.17 and 0.34 after seizure onset. We extend the statistical analysis of WFC and CFC to all subjects and obtained similar distribution.

To get insight into the evolution of synchronization between brain areas, we investigate the overall process CFC and WFC change during seizure. 60 s-length EEG signals are selected respectively in both cases: before and after seizure onset. A sliding window is applied to EEG signals and a series of PSI matrixes as Fig. 1c, d are obtained. We calculate the mean of each selected band

(23 × 23 matrix) in Fig. 3. We mainly consider the frequency bands with significant differences before and after seizure onset ($P < 0.01$). Once seizure occurs, the mean value of CFC decreases abruptly in δ–β and δ–α bands, but largely increases in θ–α bands. After about 10 s, CFC in these bands reaches its extremes quickly, and then recovers. For WFC, the synchronization level shows great increases in α, θ and δ bands, which achieves maximal values at nearly 10 s after seizure onsets. Interestingly, the change of CFC and WFC occurs earlier than seizure onset. In conclusion, the variation of PSI feature is earlier than the appearance of clinical symptoms in epileptic.

Functional brain network can directly describe the interactive integration of dynamic activities between different brain areas. The brain network of epileptic is reconstructed from PSI matrixes (Fig. 1), in which the strongest 20% links are preserved for each sub-matrix (23 × 23) in each frequency band. The selection of this threshold value can ensure the absence of isolated nodes and make sure that the difference of network before and after seizure onset is more significant. Graph theory metrics
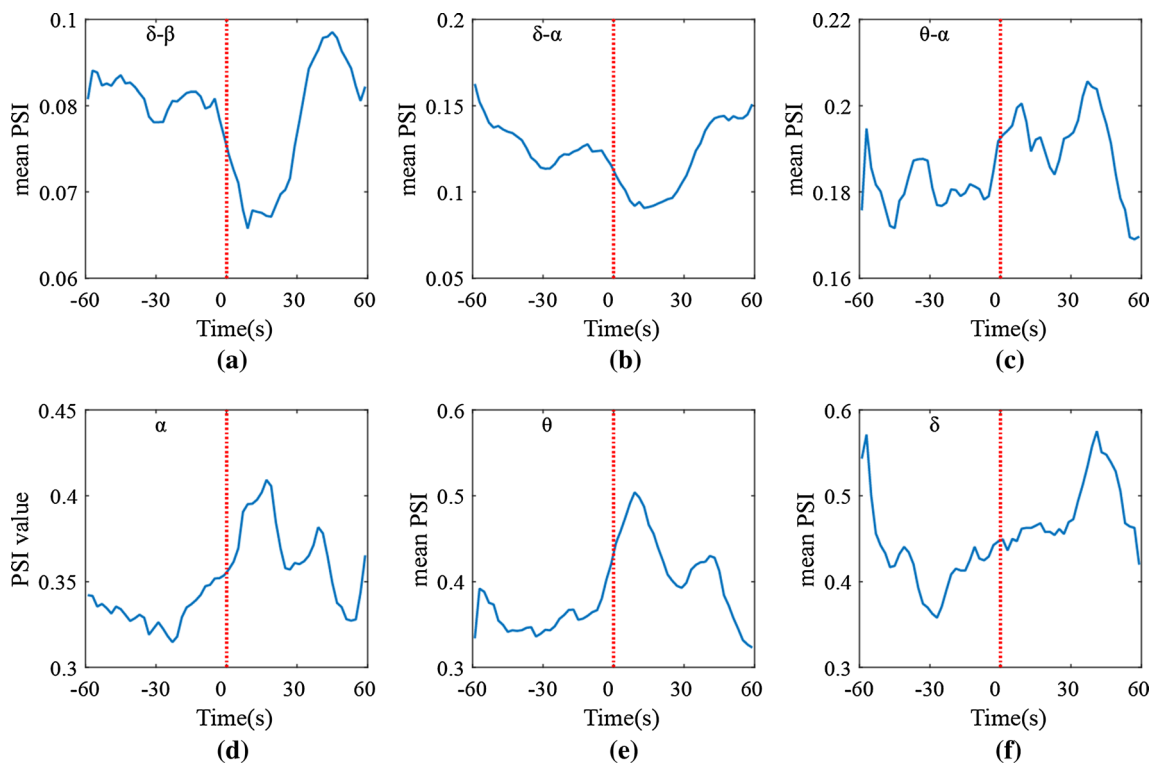
Fig. 3 Variation of mean PSI cross (**a–c**) and within (**d–f**) frequency bands during 120 s and the seizure onset (60 s) is marked with the red line. (Color figure online)

is applied to gain further insight into the CFC and WFC network properties and how it may change among different states. Several network parameters, including local efficiency and globe efficiency, are calculated in each time window of one seizure to investigate the variations of network structure before and after seizure onset. Figure 4a–h show the variations of WFC network parameters in one epileptic (same as epileptic in Fig. 2). It is obvious that when seizure occurs, the global efficiency of δ, θ and α bands declines, while there is a decline in θ band for local efficiency. We further extend statistical analysis to all subjects to explore the regular change of brain network after seizure occur. Figure 4i–l show global efficiency versus local efficiency of all subjects in WFC networks. The level of significant difference of network parameters between two states is further calculated as shown in Fig. 4i–l. The result indicates that the local network construction of epileptic brains shows no obvious change during seizure. Whereas, there is a significant decline in global network efficiency, especially in θ and α band. And the distribution of sample becomes more dispersed after seizure onset.

For CFC networks, it is observed that global efficiencies of δ–β, θ–α and δ–θ bands show descent trends once seizure occurred, and local efficiencies of δ–β, δ–α and δ–θ bands increase at the same time (Fig. 5a–l). We also extend

statistical analysis to all subjects, and find a significant difference for both local and global efficiency in δ–β, δ–α, θ–α and δ–θ bands. Figure 5m–r show structure difference of CFC networks between two states: before and after seizure onset. Compared with WFC networks (as shown in Fig. 4), the distribution of CFC samples in two cases has less overlap, indicating that CFC network may be more effective in detecting seizure onset, which is also earlier than clinical symptoms. It can be included that variation of the brain function may be due to damage in functional brain connectivity caused by seizure, which influences the integration and segregation of neural information.

Having shown significant difference of functional network for CFC and WFC case separately, we further construct two-layer network by combing the within and cross frequency PSI matrixes. For example, the 23 × 23 WFC matrixes of δ and θ bands and the 23 × 23 CFC matrixes of δ–θ and θ–δ bands are selected to combine into a 46 × 46 multi-layer PSI matrix. There is a great difference between CFC values and WFC values, hence the multi-layer network is constructed with the strongest 20% links preserved for each submatrix (23 × 23) separately (as shown in Fig. 6). Through a two-layer network, we can explore the alterations of network properties caused by the changes of both within and cross frequency coupling. Then the same analysis and network parameters are utilized to
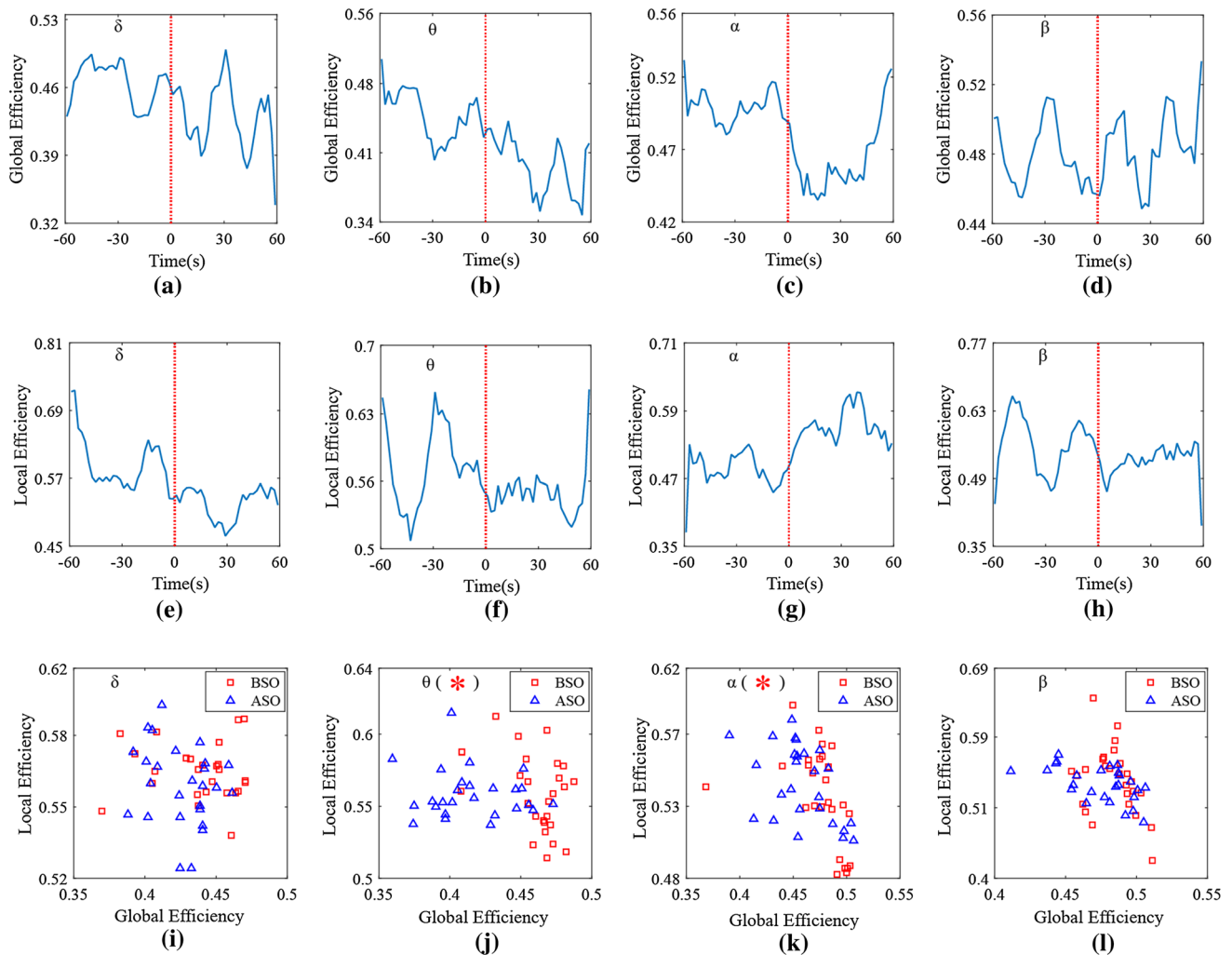
Fig. 4 **a–h** Variation of global and local efficiency of single-layered network consist of the connections within bands during 120 s and the seizure onset (60 s) is marked with the red line. **i–l** Statistical analysis of network properties variation on all subjects, where the samples before seizure onset (BSO) are represented by red squares and the samples after seizure onset (ASO) are represented by blue triangles. Red $*$ indicates a significant difference ($p < 0.05$ corrected for multiple comparisons) in global efficiency while blue $*$ represents the difference in local efficiency. (Color figure online)

investigate the variations of functional network, as shown in Fig. 7. We can observe that the global efficiency of θ–β, α–β, δ–α, θ–α, δ–θ bands all changed significant when seizure occurs. For local efficiency, there are obvious variations in α–β, δ–α, θ–α bands at the time of seizure onset. From an overall analysis perspective, both the local and global efficiency have obvious differences in θ–α, δ–θ bands between two sections (before and after seizure onset).

The density of reserved edges will affect the construction of network. In order to ensure that there is no isolated node in constructed network, at least 20% connections need to be preserved for each connectivity matrix. We also consider other proportional thresholds such as 30%, 40%, 50% and 60%, and further extract network parameters from the corresponding networks, the results are shown in

Fig. 8. It can be observed that the difference, between global efficiency and local efficiency respectively before and after seizure onset, increases with the ascension of threshold value. It suggests that in a range between 20–60%, the fewer the number of reserved edges, the more significant difference of constructed network before and after seizure onset.

Discussion

The phase synchronization is considered to be associated with active internal processing and advanced brain function (Benedek et al. 2011; Szymanski et al. 2017), and the alternation of synchronization may represent emergence and process of neuropsychiatric disorders. Ortega et al.
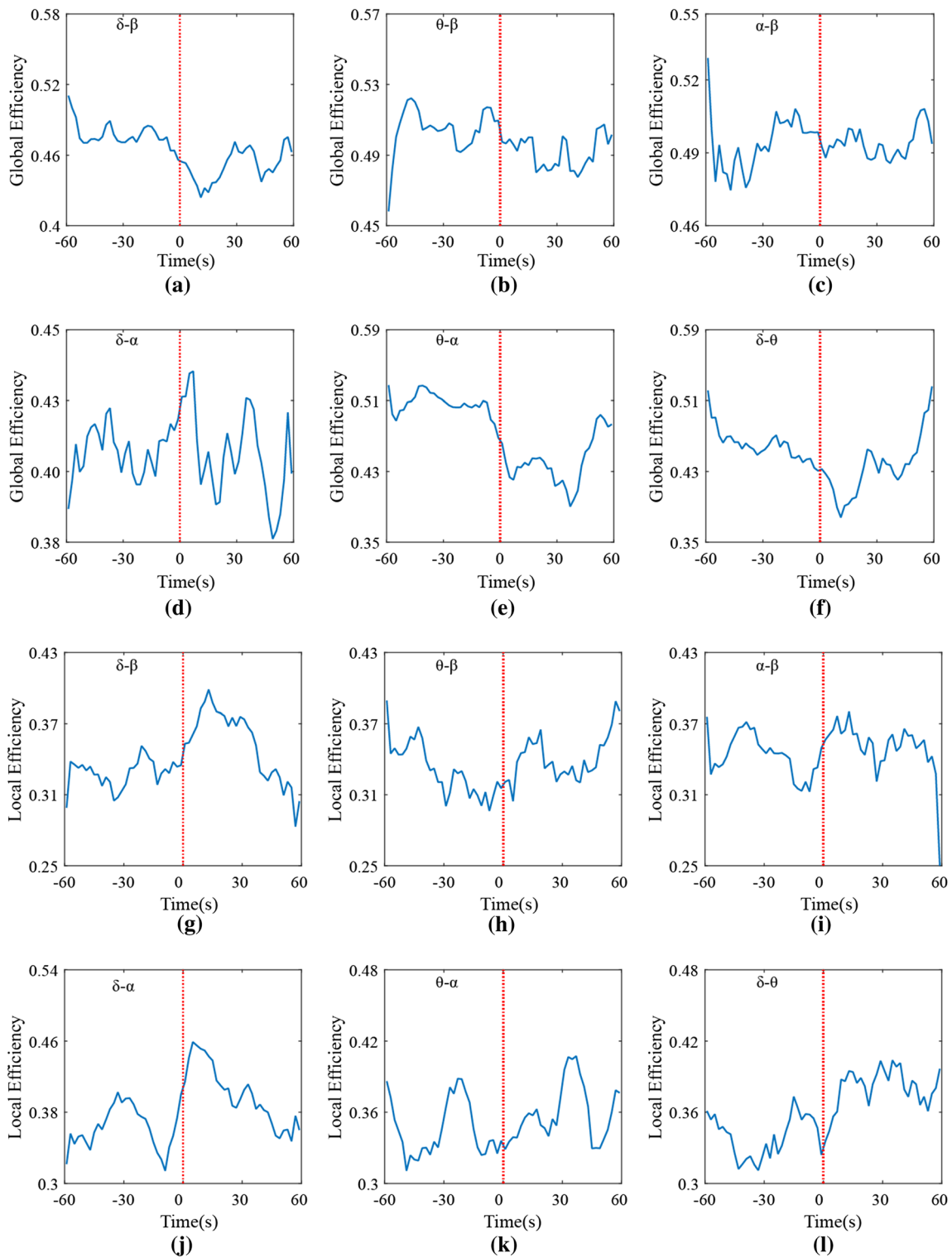
Fig. 5 **a–l** Variation of global and local efficiency of double-layered network consist of the connections between bands during 120 s and the seizure onset (60 s) is marked with the red line. **m–r** Statistical analysis of network properties variation on all subjects, where the samples BSO are represented by red squares and the samples ASO are represented by blue triangles. Red ∗ indicates a significant difference ($p < 0.05$ corrected for multiple comparisons) in global efficiency while blue ∗ represents the difference in local efficiency. (Color figure online)
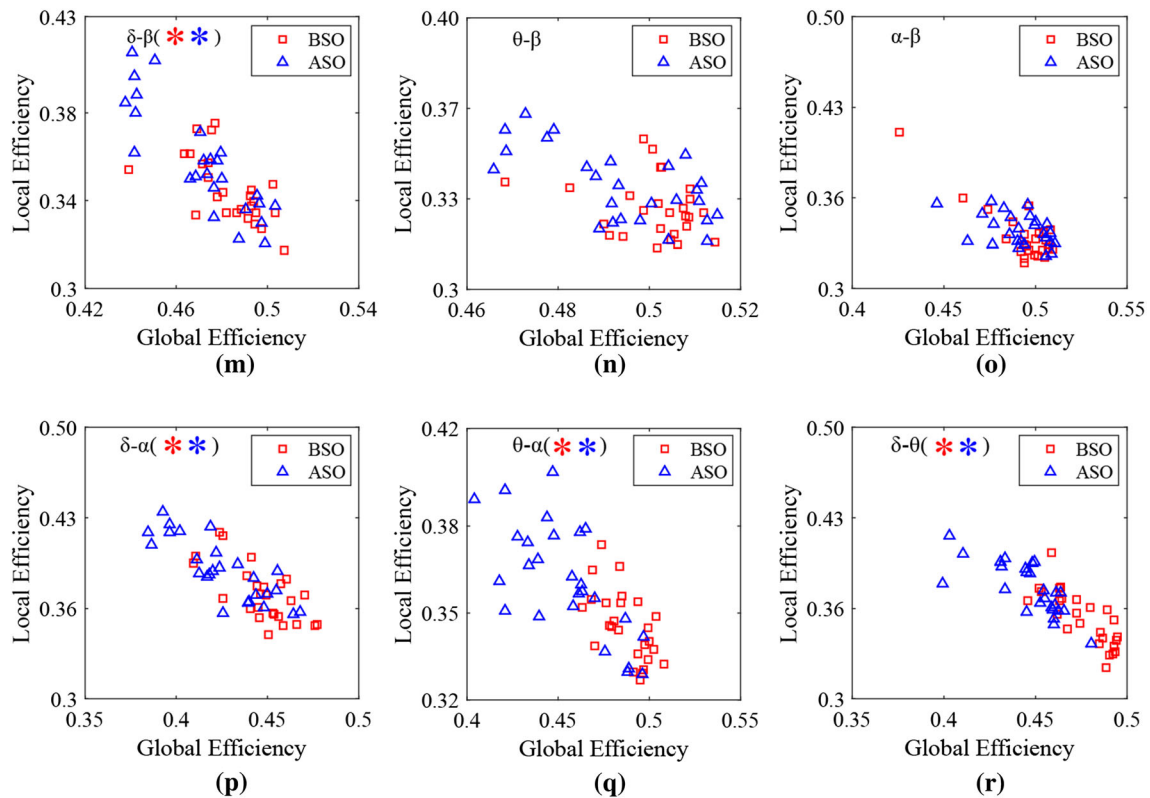
Fig. 5 continued

Fig. 6 Schematic presentation of the multi-layer network constructed by CFC and WFC between θ and α bands. The red lines indicate the preserved connectivity within specific bands, while the yellow lines represent the connectivity between different bands. (Color figure online)
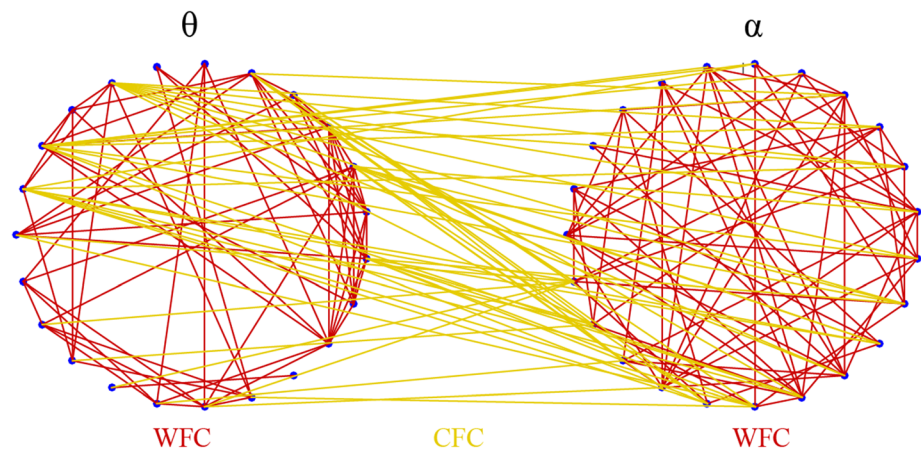

(2008) studied the synchronous activity emerges from lateral intracortical regions and proved that phase synchronization could be utilized to locate the specific cortical sites that were closely related to epilepsy seizure. In addition, researchers generally concentrated on the coupling between neurons of different brain regions while ignored the fact that electrical signals of different frequencies correspond to different consciousness states of brain in earlier studies (Amiri et al. 2016; Palva and Palva 2018).

Another study demonstrated that cross-frequency phase synchrony, existed in cortical oscillations and could serve

Fig. 7 a–l Variation of global and local efficiency of one subject's ▶ global brain network constructed by all the connections within and between bands during 120 s and the seizure onset (60 s) is marked with red line. **m–r** Statistical analysis of network properties variation on all subjects, where the samples BSO are represented by red squares and the samples ASO are represented by blue triangles. Red $*$ indicates a significant difference ($p < 0.05$ corrected for multiple comparisons) of global efficiency while blue $*$ represents the difference of local efficiency. (Color figure online)

to integrate, coordinate and regulate neuronal processing distributed into neuronal assemblies concurrently in multiple frequency bands (Palva and Palva 2018). There were a
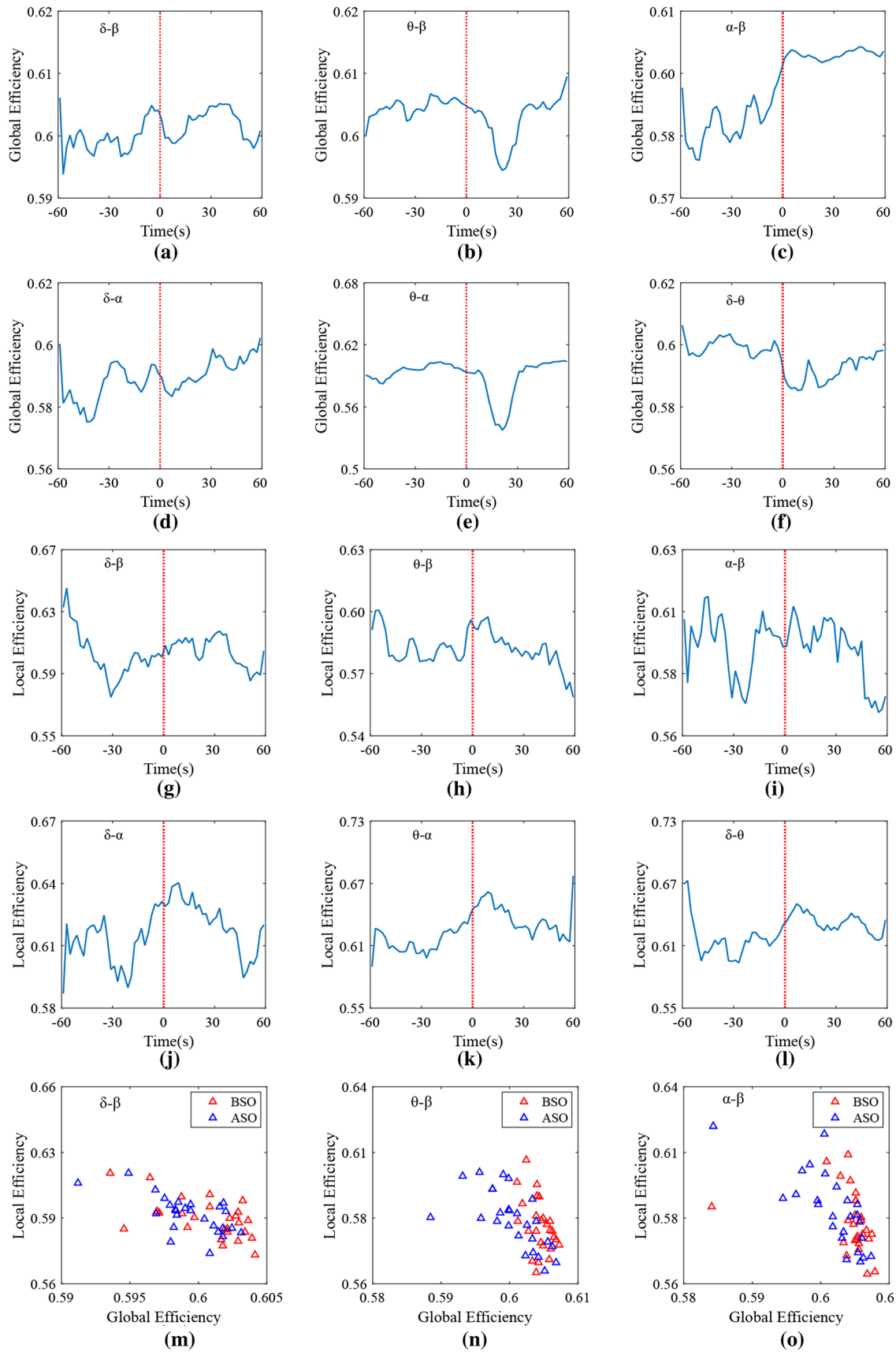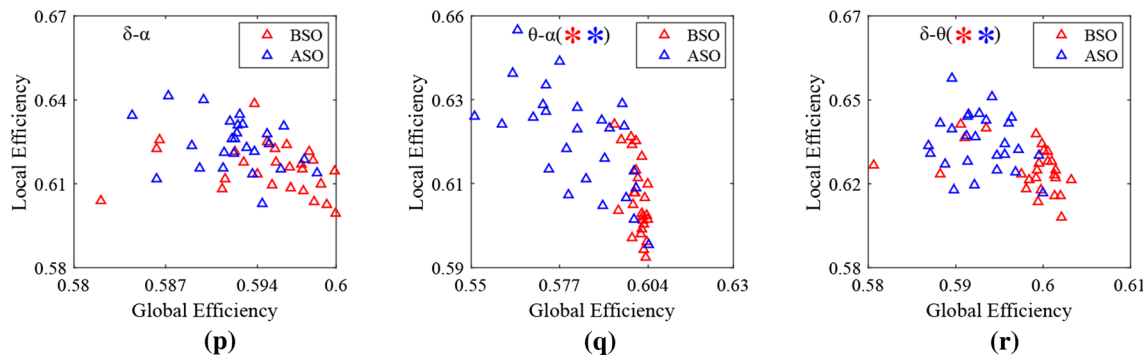
Fig. 7 continued

number of metrics for functional across coupling, like phase-amplitude coupling (PAC), phase–phase coupling (PPC), and amplitude–amplitude coupling (AAC). Amiri et al. reported that the PAC between high and low frequency bands in patients with focal epilepsy was significantly stronger in the seizure-onset zone (SOZ) compared to normal regions (Amiri et al. 2016; Kim et al. 2018). Another study also used the PAC method and found that coupling was more regularly inside than outside the SOZ (Weiss et al. 2016). Moreover, a recent study has explored the amplitude–amplitude modulation and revealed that variations of δ–θ and δ–β coupling were both related to the severity of Alzheimer (Fraga et al. 2013). This seemed feasible to apply the cross-frequency coupling in differentiation and detection of neurological diseases. However, PAC shows low confidence of the results especially under the influence of noises. Besides, PAC analysis on the modulation relationship between different frequency bands is mainly limited to one channel. Thus, problems may come out when considering between frequency band interactions. Hence, we apply PSI to detect and quantify the statistical coupling both within and between different frequency bands in EEG data. The PSI matrix may offer unique insights into how the brain employs different regions to communicate and collaborate for information processing, especially in different frequency bands (Englot et al. 2018).

Previous research has shown large-scale neuronal synchronization is the potential mechanism underlying seizure generation and the properties of phase synchronization change radically depending on the connectivity structure of the network (Fraga et al. 2013; Ponten et al. 2007; Reijneveld et al. 2007). In addition, the functional segregation and integration of brain networks, which can be represented by local and global efficiency, is deemed to be less balanced in epileptics. Hence, we further construct the global brain network through PSI matrix, and extract the graph theory metrics to explore the properties of brain networks constructed by the coupling within and cross

frequency bands. We have found that the epileptic networks show a decrease of global efficiency within θ band when seizure occurs. Previous studies showed that mean clustering coefficient and global efficiency in the patients with epilepsy had strong tendency to decrease, compared to those in healthy subjects (Song et al. 2015). Several other studies have found the similar decreases of global efficiency of epileptic brain in the β band (Jacobs et al. 2018), which is also in accordance with our results in view of the change of network properties. The disruption of global efficiency in epilepsy patients suggest a decline of efficiency for global information transmission after seizure onset, which may be the cause of sensory disturbances and loss of consciousness in patients. On the other side, considering the cross frequency interactions, we found that it showed elevated local efficiency properties and decreased global efficiency properties in δ–β, δ–α, δ–θ and θ–α networks. The changed cross functional network might be due to the loss of long-range connectivity between different sub-networks with excessive synchronization within them. We further constructed a two-layer network, which may help to mediate simultaneous formation of multiple brain networks, to observe the alteration of network properties caused by the change of both within and cross frequency coupling. The results are broadly consistent with those of CFC network, indicating that the altered functional connectivity between bands in epileptic brain may play an important role in emergence of the disease.

Phase synchronization between different bands we observed may change drastically when seizure occurs, with the structure of reconstructed multi-layer network altered. The findings support previous evidence that cross-frequency coupling might be the key element in detection and diagnosis of epilepsy. In addition, we have found the alterations of cross frequency connectivity strength and network structure are both earlier than the appearance of clinical symptoms in seizure. It suggests that epilepsy might be predicted through monitoring the phase synchronization between and within frequency bands.
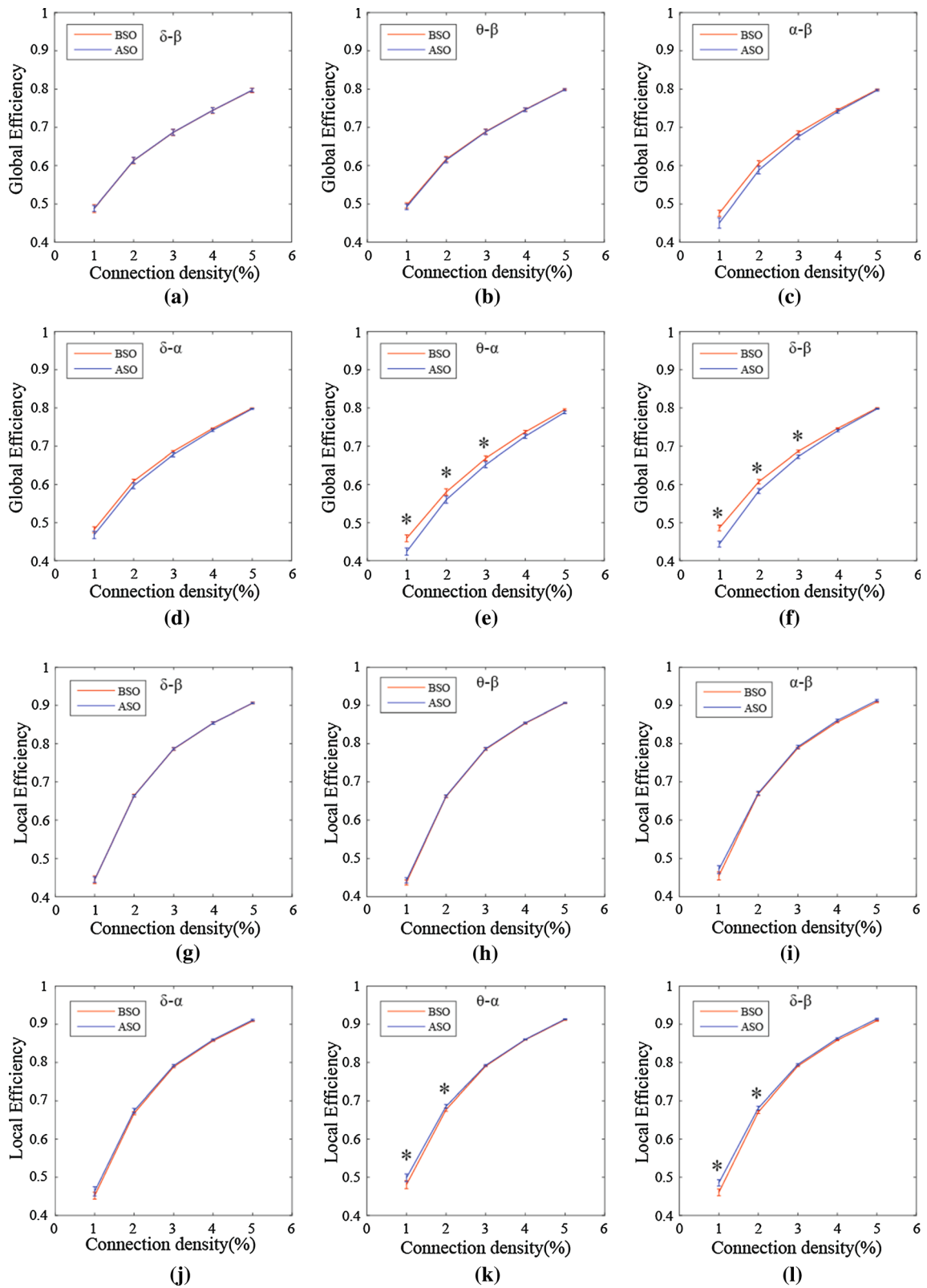
Fig. 8 Mean and standard deviation of global efficiency (**a–f**) and mean local efficiency (**g–l**) of one subject's multi-layer network under different threshold values for different frequency bands. Black * indicates a significant difference ($p < 0.05$ corrected for multiple comparisons) in global or local efficiency at a certain connection density

However, it needs to be noted that we make an exploratory analysis in a small group at a total of 22 subjects. Besides, the EEG data derived from pediatric subjects suffering from intractable seizures without a specific classification on the types of epilepsy. Future research will replicate the results with another bigger patient cohort and investigate whether other neurologic diseases can show similar phenomena considering the cross-frequency interaction.

Conclusions

In this work, we have considered the cross-frequency coupling and functional brain networks of epileptic. Through PSI, a measure quantifying the synchronization strength within and between separate frequency bands of EEG, significant differences between interictal and ictal states can be observed in both WFC and CFC cases. Specifically, the synchronization strength is significantly increased within δ, θ and α bands from interictal to ictal state. For the CFC case, a significant increase is found for the θ–α and δ–α couplings together with a decline for δ–β couplings. Through the synchronization index calculated every 3 s with an overlap of 2 s, we can also find that the variations of connectivity may precede the appearance of clinical symptoms in epileptic. Furthermore, we reconstruct the brain network by the connections within and cross frequencies by PSI matrixes, and calculate local efficiency and globe efficiency to investigate the properties of brain network. There is no obvious changes in global efficiency, whereas local efficiency shows a significant decline in θ band. For CFC networks, we have found a significant decrease for local efficiency and a significant increase for global efficiency in δ–β, δ–α, θ–α and δ–θ networks.

References

Abasolo D, Hornero R, Espino P, Poza J, Sanchez CI, de la Rosa R (2005) Analysis of regularity in the EEG background activity of Alzheimer's disease patients with approximate entropy. Clin Neurophysiol 116(8):1826–1834

Adebimpe A, Aarabi A, Bourel-Ponchel E, Mahmoudzadeh M, Wallois F (2016) EEG resting state functional connectivity analysis in children with benign epilepsy with centrotemporal spikes. Front Neurosci 10:143

Amiri M, Frauscher B, Gotman J (2016) Phase–amplitude coupling is elevated in deep sleep and in the onset zone of focal epileptic seizures. Front Hum Neurosci 10:387

Apkarian AV, Bushnell MC, Treede RD, Zubieta JK (2005) Human brain mechanisms of pain perception and regulation in health and disease. Eur J Pain 9(4):463–484

Belluscio MA, Mizuseki K, Schmidt R, Kempter R et al (2012) Cross-frequency phase–phase coupling between θ and γ oscillations in the hippocampus. J Neurosci 32(2):423–435

Benbadis SR, Allen Hauser W (2000) An estimate of the prevalence of psychogenic non-epileptic seizures. Seizure 9(4):280–281

Benedek M, Bergner S, Koenen T, Fink A, Neubauer AC (2011) EEG α synchronization is related to top-down processing in convergent and divergent thinking. Neuropsychologia 49(12):3505–3511

Biswal B, Yetkin FZ, Haughton VM, Hyde JS (1995) Functional connectivity in the motor cortex of resting human brain using echo-planar MRI. Magn Reson Med 34(4):537–541

Buckner RL, Sepulcre J, Talukdar T et al (2009) Cortical hubs revealed by intrinsic functional connectivity: mapping, assessment of stability, and relation to Alzheimer's disease. J Neurosci 29(6):1860–1873

Cai LH, Wei XL, Wang J, Yu HT, Deng B, Wang R (2018) Reconstruction of functional brain network in Alzheimer's disease via cross-frequency phase synchronization. Neurocomputing 314:490–500

Canolty RT, Knight RT (2010) The functional role of cross-frequency coupling. Trends Cogn Sci 14(11):506–515

Donos C, Dumpelmann M, Schulze-Bonhage A (2015) Early seizure detection algorithm based on intracranial EEG and random forest classification. Int J Neural Syst 25(5):1550023

Edakawa K, Yanagisawa Kishima H, Fukuma R, Oshino S, Khoo HM et al (2016) Detection of epileptic seizures using phase–amplitude coupling in intracranial electroencephalography. Sci Rep 6:25422

Englot DJ, Gonzalez HFJ, Reynolds BB, Konrad PE, Jacobs ML, Gore JC, Landman BA, Morgan VL (2018) Relating structural and functional brainstem connectivity to disease measures in epilepsy. Neurology 91:e67–e77

Fraga FJ, Falk TH, Kanda PA, Anghinah R (2013) Characterizing Alzheimer's disease severity via resting-awake EEG amplitude modulation analysis. PLoS ONE 8(8):e72240

Greter H, Mmbando B, Makunde W, Mnacho M, Matuja W, Kakorozya A, Suykerbuyk P, Colebunders R (2018) Evolution of epilepsy prevalence and incidence in a Tanzanian area endemic for onchocerciasis and the potential impact of community-directed treatment with ivermectin: a cross-sectional study and comparison over 28 years. BMJ Open 8(3):e017188

Guirgis M, Chinvarun Y, del Campo M, Carlen PL, Bardakjian BL (2015) Defining regions of interest using cross-frequency coupling in extratemporal lobe epilepsy patients. J Neural Eng 12(2):026011

Hortal E, Ubeda A, Ianez E, Azorin JM, Fernandez E (2016) EEG-based detection of starting and stopping during gait cycle. Int J Neural Syst 26(7):1650029

Iasemidis LD, Shiau DS, Chaovalitwongse W et al (2003) Adaptive epileptic seizure prediction system. IEEE Trans Biomed Eng 50(5):616–627

Ibrahim GM, Wong SM, Anderson RA et al (2014) Dynamic modulation of epileptic high frequency oscillations by the phase of slower cortical rhythms. Exp Neurol 251:30–38

Jacobs D, Hilton T, del Campo M, Carlen PL, Bardakjian BL (2018) Classification of pre-clinical seizure states using scalp EEG cross-frequency coupling features. IEEE Trans Biomed Eng 65(11):2440–2449

Jeong W, Jin SH, Kim M, Kim JS, Chung CK (2014) Abnormal functional brain network in epilepsy patients with focal cortical dysplasia. Epilepsy Res 108(9):1618–1626

Jiang YZ, Wu DR, Deng ZH et al (2017) Seizure classification from EEG signals using transfer learning, semi-supervised learning and TSK fuzzy system. IEEE Trans Neural Syst Rehabil Eng 25(12):2270–2284

Kannathal N, Choo ML, Acharya UR et al (2005) Entropies for detection of epilepsy in EEG. Comput Methods Programs Biomed 80(3):187–194

Kim HJ, Lee JH, Park CH, Hong HS, Choi YS, Yoo JH, Lee HW (2018) Role of language-related functional connectivity in patients with benign childhood epilepsy with centrotemporal spikes. J Clin Neurol 14:48–57

Kirmani BF (2013) Importance of video-EEG monitoring in the diagnosis of epilepsy in a psychiatric patient. Case Rep Neurol Med 2013:159842

Liao W, Zhang Z, Pan Z et al (2010) Altered functional connectivity and small-world in mesial temporal lobe epilepsy. Epilepsy Res 137:45–52

Lo JT (2010) Functional model of biological neural networks. Cogn Neurodyn 4(4):295–313

Malladi R, Johnson DH, Kalamangalam GP, Tandon N, Aazhang B (2018) Mutual information in frequency and its application to measure cross-frequency coupling in epilepsy. IEEE Trans Signal Process 66(11):3008–3023

Martis RJ, Acharya UR, Tan JH et al (2013) Application of intrinsic time-scale decomposition (ITD) to EEG signals for automated seizure prediction. Int J Neural Syst 23(5):1350023

Medvedev AV, Murro AM, Meador KJ (2011) Abnormal interictal gamma activity may manifest a seizure onset zone in temporal lobe epilepsy. Int J Neural Syst 21(2):103–114

Mormann F, Lehnertz K, David P, Elger CE (2000) Mean phase coherence as a measure for phase synchronization and its application to the EEG of epilepsy patients. Physica D 144(3–4):358–369

Müller V, Perdikis D, Oertzen TV et al (2016) Structure and topology dynamics of hyper-frequency networks during rest and auditory oddball performance. Front Comput Neurosci 10:108

Nariai H, Matsuzaki N, Juhasz C et al (2011) Ictal high-frequency oscillations at 80–200 Hz coupled with δ phase in epileptic spasms. Epilepsia 52(10):e130–e134

Nishida H, Takahashi M, Lauwereyns J (2014) Within-session dynamics of θ-gamma coupling and high-frequency oscillations during spatial alternation in rat hippocampal area CA1. Cogn Neurodyn 8(5):363–372

Ortega GJ, Menendez de la Prida L, Sola RG, Pastor J (2008) Synchronization clusters of interictal activity in the lateral temporal cortex of epileptic patients: intraoperative electrocorticographic analysis. Epilepsia 49(2):269–280

Palva JM, Palva S (2018) Functional integration across oscillation frequencies by cross-frequency phase synchronization. Eur J Neurosci 48(7):2399–2406

Percha B, Dzakpasu R, Zochowski M, Parent J (2005) Transition from local to global phase synchrony in small world neural network and its possible implications for epilepsy. Phys Rev E Stat Nonlinear Soft Matter Phys 72(3 Pt 1):031909

Ponten SC, Bartolomei F, Stam CJ (2007) Small-world networks and epilepsy: graph theoretical analysis of intracerebrally recorded mesial temporal lobe seizures. Clin Neurophysiol 118(4):918–927

Ponten SC, Douw L, Bartolomei F, Reijneveld JC, Stam CJ (2009) Indications for network regularization during absence seizures:

weighted and unweighted graph theoretical analyses. Exp Neurol 217(1):197–204

Qu J, Wang R, Du Y, Cao J (2012) Synchronization study in ring-like and grid-like neuronal networks. Cogn Neurodyn 6(1):21–31

Reijneveld JC, Ponten SC, Berendse HW, Stam CJ (2007) The application of graph theoretical analysis to complex networks in the brain. Clin Neurophysiol 118(11):2317–2331

Rogasch NC, Fitzgerald PB (2013) Assessing cortical network properties using TMS-EEG. Hum Brain Mapp 34(7):1652–1669

Roper SN, Yachnis AT (2002) Cortical dysgenesis and epilepsy. Neuroscientist 8(4):356–371

Salvador R, Suckling J, Schwarzbauer C, Bullmore E (2005) Undirected graphs of frequency-dependent functional connectivity in whole brain networks. Philos Trans R Soc Lond B Biol Sci 360(1457):937–946

Samiee S, Levesque M, Avoli M, Baillet S (2018) Phase-amplitude coupling and epileptogenesis in an animal model of mesial temporal lobe epilepsy. Neurobiol Dis 114:111–119

Song J, Nair VA, Gaggl W, Prabhakaran V (2015) Disrupted brain functional organization in epilepsy revealed by graph theory analysis. Brain Connect 5(5):276–283

Srinivas KV, Jain R, Saurav S, Sikdar SK (2007) Small-world network topology of hippocampal neuronal network is lost, in an in vitro glutamate injury model of epilepsy. Eur J Neurosci 25(11):3276–3286

Szymanski C, Pesquita A, Brennan AA et al (2017) Teams on the same wavelength perform better: inter-brain phase synchronization constitutes a neural substrate for social facilitation. Neuroimage 152:425–436

Tecchio F, Cottone C, Porcaro C, Cancelli A, Di Lazzaro V, Assenza G (2018) Brain functional connectivity changes after transcranial direct current stimulation in epileptic patients. Front Neural Circuits 12:44

Tetzlaff R, Kunz R, Niederhofer C (2003) Cellular neural networks (CNN) with linear weight functions for a prediction of epileptic seizures. Int J Neural Syst 13(6):489–498

Thuraisingham RA, Tran Y, Craig A et al (2012) Frequency analysis of eyes open and eyes closed EEG signals using the Hilbert-Huang transform. IEEE Eng Med Biol Soc 2012:2865–2868

Villa AE, Tetko IV (2010) Cross-frequency coupling in mesiotemporal EEG recordings of epileptic patients. J Physiol Paris 104(3–4):197–202

Wacker M, Witte H (2011) On the stability of the n:m phase synchronization index. IEEE Trans Biomed Eng 58(2):332–338

Wang B, Meng L (2016) Functional brain network alterations in epilepsy: a magnetoencephalography study. Epilepsy Res 126:62–69

Weiss SA, Banks GP, McKhann GM Jr et al (2013) Ictal high frequency oscillations distinguish two types of seizure territories in humans. Brain 136(Pt 12):3796–3808

Weiss SA, Orosz I, Salamon N et al (2016) Ripples on spikes show increased phase-amplitude coupling in mesial temporal lobe epilepsy seizure-onset zones. Epilepsia 57(11):1916–1930

Yuan SS, Zhou WD, Chen LY (2018) Epileptic seizure prediction using diffusion distance and bayesian linear discriminate analysis on intracranial EEG. Int J Neural Syst 28(1):1750043

Zhang Y, Zhou W, Yuan S et al (2015) Seizure detection method based on fractal dimension and gradient boosting. Epilepsy Behav 43:30–38

Zheng CG, Zhang T (2013) Alteration of phase-phase coupling between θ and gamma rhythms in a depression-model of rats. Cogn Neurodyn 7(2):167–172

Publisher's Note Springer Nature remains neutral with regard to jurisdictional claims in published maps and institutional affiliations.